THE JOURNAL OF BIOLOGICAL CHEMISTRY VOL. 288, NO. 22, pp. 15481–15494, May 31, 2013

Induction of C-X-C Chemokine Receptor Type 7 (CXCR7) Switches Stromal Cell-derived Factor-1 (SDF-1) Signaling and Phagocytic Activity in Macrophages Linked to Atherosclerosis*

Received for publication, December 14, 2012, and in revised form, April 15, 2013 Published, JBC Papers in Press, April 18, 2013, DOI 10.1074/jbc.M112.445510

Wanshu Ma, Yiwei Liu, Nicholas Ellison, and Jianzhong Shen[1]

From the Division of Pharmacology, Department of Pharmacal Sciences, Harrison School of Pharmacy, Auburn University, Auburn, Alabama 36849

Background: Previously, whether the new SDF-1 receptor CXCR7 plays a role in macrophages linked to disease was unknown.
Results: During macrophage differentiation, CXCR7 is up-regulated, detected in mouse atherosclerotic plaques, and mediates pro-phagocytic activity via JNK and p38 pathways.
Conclusion: CXCR7 is a functional SDF-1 receptor in macrophages.
Significance: Macrophage CXCR7 might be a new therapeutic target for atherosclerosis.

The discovery of CXCR7 as a new receptor for SDF-1 places many previously described SDF-1 functions attributed to CXCR4 in question, though whether CXCR7 acts as a signaling or "decoy" receptor has been in debate. It is known that CXCR7 is not expressed in normal blood leukocytes; however, the potential role of leukocyte CXCR7 in disease states has not been addressed. The aim of this study was to determine the expression and function of macrophage CXCR7 linked to atherosclerosis. Here, we show that CXCR7 was detected in macrophage-positive area of aortic atheroma of ApoE-null mice, but not in healthy aorta. During monocyte differentiation to macrophages, CXCR7 was up-regulated at mRNA and protein levels, with more expression in M1 than in M2 phenotype. In addition, CXCR7 induction was associated with a SDF-1 signaling switch from the pro-survival ERK and AKT pathways in monocytes to the pro-inflammatory JNK and p38 pathways in macrophages. The latter effect was mimicked by a CXCR7-selective agonist TC14012 and abolished by siRNA knockdown of CXCR7. Furthermore, CXCR7 activation increased macrophage phagocytic activity, which was suppressed by CXCR7 siRNA silencing or by inhibiting either the JNK or p38 pathways, but was not affected by blocking CXCR4. Finally, activation of CXCR7 by I-TAC showed a similar signaling and phagocytic activity in macrophages with no detectable CXCR3. We conclude that CXCR7 is induced during monocyte-to-macrophage differentiation, which is required for SDF-1 and I-TAC signaling to JNK and p38 pathways, leading to enhanced macrophage phagocytosis, thus possibly contributing to atherogenesis.

Atherosclerotic cardiovascular disease is the leading cause of morbidity and mortality worldwide. Although lipid-lowering drugs have had great success, they fail to protect more than half of patients from cardiovascular events (1). Thus, there is a need for additional pharmacological targets for new treatment options. It is well established that monocyte-derived macrophages are prevalent in atherosclerotic lesions of patients (2). Therefore, intervention of monocyte recruitment to the building plaques may constitute a viable strategy to reduce plaque macrophage burden, thereby improving clinical success in combating atherosclerotic diseases (3).

Monocyte/macrophage infiltration into the vascular wall is controlled by many factors including those from the chemokine family. Among the ~40 human chemokines, the majority were pro-atherogenic (4). However, conflicting results were reported for the role of stromal cell-derived factor (SDF)[2]-1 (also termed CXCL12) in atherosclerosis, with both pro- & anti-atherogenic effects suggested (4–7). For a long time, it was accepted that SDF-1 exclusively binds to CXCR4 (8). However, recent deorphanization of CXCR7 as a new high affinity receptor for SDF-1 places many cellular functions previously attributed to CXCR4 in question (9). Studies in gene knock-out mice indicate that CXCR4, but not CXCR7, is required for hematopoiesis (10, 11). Consistent with this, a recent study demonstrated that CXCR7 is not expressed in normal human or mouse blood leukocytes. (12) However, the potential role of leukocyte CXCR7 in disease states has not been addressed.

Our previous work, along with others, showed that in *ApoE*-null mice or humans with atherosclerosis, plasma SDF-1 level is significantly lower than normal (13, 14). In contrast, SDF-1 is not detected in healthy arteries, but is highly expressed in atherosclerotic plaques (4). These findings suggest a potential "healthy" SDF-1 gradient across the vascular wall, which is

* This study was supported by the New Faculty Startup Fund Auburn University (to J. S.) and the American Heart Association-National SDG Award 12SDG8850011 (to J. S.).
[1] To whom correspondence should be addressed: Division of Pharmacology, Department of Pharmacal Sciences, Auburn University-School of Pharmacy, 4306G Walker Building, Auburn, AL 36849. Tel.: (334)-844-8118; Fax: (334)-844-8331; E-mail: jzs0019@auburn.edu.

[2] The abbreviations used are: SDF, stromal cell-derived factor; LPS, lipopolysaccharide; PBMC, peripheral blood mononuclear cell; PMA, phorbol 12-myristate 13-acetate; DAPI, 4′,6-diamidino-2-phenylindole.

reversed in atherosclerosis. Intrigued by these considerations, we were interested in exploring whether CXCR7 expression may follow the same pattern of change as its agonist SDF-1 in the context of atherosclerosis.

Thus, the principle objective of this study was to determine whether CXCR7 is expressed in macrophage-enriched atherosclerotic plaques, and if so, which macrophage signaling pathways are specifically activated by CXCR7. Secondly, we sought to determine whether CXCR7 induction promotes macrophage phagocytosis.

EXPERIMENTAL PROCEDURES

Cell Culture, Differentiation, and Stimulation—Human THP-1 monocytic cells (ATCC) were cultured in RPMI 1640 (HyClone, Thermo) supplemented with 10% heat-inactivated fetal bovine serum (FBS) (HyClone, Thermo), 100 units/ml penicillin, and 100 μg/ml streptomycin (Lonza) at 37 °C in a humidified atmosphere with 5% CO_2.

For the induction of cell differentiation, THP-1 cells were seeded at 5×10^5 cells/well in six-well plates in RPMI 1640 supplemented with 5% FBS with 40 nM PMA for 48 h or otherwise indicated times. Alternatively, THP-1 cells were stimulated for 24 h with IFN-γ (100 ng/ml) and M-CSF (10 ng/ml) or with IFN-γ (100 ng/ml) and LPS (1 μg/ml). The non-adherent cells were removed by aspiration. Before agonist stimulation, differentiating THP-1 macrophages were starved for 10 h in RPMI 1640 without FBS, and this starvation did not change CXCR7 mRNA expression as compared with non-starved cells (data not shown). Potential endogenous SDF-1 secreted by macrophages was minimized by changing the starvation medium 2 h before the end of starvation. Cells were pretreated with inhibitors or antagonists for 40 min before stimulation.

To obtain polarized human macrophages, blood primary monocytes were differentiated into M1 or M2 phenotype by treatment of the cells with the following different reagents for 48 h: IFN-γ (100 ng/ml)+LPS (1 μg/ml), M-CSF (20 ng/ml)+LPS(1 μg/ml), GM-CSF (50 ng/ml)+ LPS(1 μg/ml), IL-4 (20 ng/ml), or IL-13 (20 ng/ml).

Isolation of Human Primary Blood Monocytes—Human peripheral blood mononuclear cells (PBMCs) were separated from Buffy Coat (*Biological Specialty Corp*) by density-gradient centrifugation on Histopaque-1077 (Sigma). The investigation conforms to the principles outlined in the Declaration of Helsinki for use of human tissue or subjects, and was approved by Auburn University, Office of Human Subjects Research. Untouched human primary monocytes were purified by negative selection using a Dynabeads kit (Invitrogen), yielding an average 98% purity. Freshly isolated monocytes were cultured in RPMI 1640 supplemented with 10% heat-inactivated FBS and antibiotics and used in experiments after being stabilized for at least 2 h. Unless otherwise specified in the figures or figure legends, all human primary macrophages were induced into M1 phenotype by IFN-γ (100 ng/ml)+LPS (1 μg/ml) for 2~3 days before cell signaling and phagocytosis assays.

RT-PCR Analysis—The total RNA and DNA were extracted from THP-1 cells, human primary monocytes and THP-1-derived macrophages according to manufacturer's protocol for the RNeasy and DNeasy kits, respectively (Qiagen). For the synthesis of the first strand of cDNA, 1 μg of total RNA after DNase (Ambion) treatment was reverse-transcribed using a cDNA synthesis kit (Applied Biosystems). The cDNA samples were then amplified by PCR using 2.5 units of TaqDNA polymerase (Roche Applied Science). The PCR amplification was performed with jump start for 2 min at 95 °C, followed by 40 thermal cycles of denaturation for 1 min at 95 °C, annealing for 1 min at 56 °C, and extension at 72 °C for 1 min with a final extension at 72 °C for 10 min. The resulting PCR products were resolved on a 1.5% agarose ethidium bromide gel, and the bands were visualized with ultraviolet light as we previously reported (13).

Real-time PCR Analysis—Real-time RT-PCR was carried out using an iCycler iQ5 detection system (Bio-Rad) with SYBR Green reagents (Applied Biosystems), as we previously described (13). The PCR mixture (20 μl) contained 0.5 μM concentration of each primer, 4 μl of water, 10 μl of SYBR Green mixture, and 5 μl of cDNA. The samples were placed and sealed in 96-well plates with the following reaction condition: initial PCR activation step (5 min at 95 °C), and cycling steps (denaturation for 1 min at 95 °C, annealing for 1 min at 60 °C, extension for 2 min at 72 °C; 40 cycles). An internal control, GAPDH, was amplified in separate wells. The threshold cycle (Ct) value and the efficiency of PCR amplification for each set of primers were determined using the accompanying software. We used the comparative cycle threshold $\Delta\Delta$Ct method for relative quantification of gene expression. The sequences of primers are: human CXCR4: Forward: 5′-CACTTCAGATAACTACACCG-3′, and Reverse: 5′-ATCCAGACGCCAACATAGAC-3′; human CXCR7: Forward: 5′-TGGTCAGTCTCGTGCAGCAC-3′, and Reverse: 5′-GCCAGCAGACAAGGAAGACC-3′; human GAPDH: Forward: 5′-TCAACAGCGACACCCACTCC-3′, and Reverse: 5′-TGAGGTCCACCACCCTGTTG-3′.

Western Blotting—After stimulation for indicated times, cells were lysed, and standard Western blotting was performed as previously described (13). The individual primary antibodies used were: mouse monoclonal anti-hCXCR7 (clone 11G8, R&D Systems; clone 9C4, MBL; clone 8F11-M16, BioLegend), mouse monoclonal anti-hCXCR4 (clone 12G5, R&D Systems), anti-p-ERK, anti-p-p38, anti-p-JNK, and anti-p-AKT (1:1000, Cell Signaling). Equal protein loading was verified by stripping off the original antibodies and re-probing the membranes with the primary antibody β-actin, GAPDH, tubulin, or total ERK1/2, p38, or JNK (1:1000).

Immunofluorescence Assay—THP-1 cells and primary human blood monocytes were seeded in 8-chamber glass slides (Nunc) with or without differentiation into macrophages. After 48 h, the medium was aspirated, and cells were fixed for 10 min in cold methanol. The fixed cells were washed with PBS three times and blocked with 3% horse serum for 1 h at room temperature. Then the cells were incubated with mouse monoclonal anti-hCXCR7 antibody (1:100, 11G8) overnight at 4 °C followed by incubation with FITC-conjugated anti-mouse IgG for 90 min at room temperature in darkness. For negative controls, cells were incubated with non-immune IgG in place of the specific primary antibody or just the FITC-conjugated secondly antibody. Images with fluorescent signals in random fields were acquired and captured using an AMG EVOS® digital inverted

multi-functional microscope (AMG) as we previously reported (13).

Flow Cytometry Assay—For determining cell surface CXCR4, CXCR7, CXCR3, CD36, and CD206 (macrophage mannose receptor), cells were washed twice with flow cytometry staining buffer and suspended in the same buffer to a final concentration of 4×10^6 cells/ml. Then, 25-μl cell aliquots were transferred for Fc receptor blocking with human IgG for 15 min at room temperature. Cells were stained with PE-conjugated anti-human CXCR7 (11G8), fluorescein-conjugated anti-human CXCR4 (12G5), PE-conjugated anti-human CXCR3 (BD Pharmingen), FITC-conjugated anti-human CD36 (BioLegend), Alexa Fluor 488-conjugated anti-human CD206 (BioLegend), or non-immune IgG isotype controls at 10 μg/ml on ice for 30 min in darkness and then rinsed with cold buffer (PBS containing 2% FBS). For intracellular staining of CD68, cells were washed twice with flow cytometry staining buffer and fixed for 10 min at room temperature in 4% paraformaldehyde. After two washes, cells were resuspended in 100 μl of 0.5% Triton X-100 in PBS buffer plus 0.5 μg/ml FITC-labeled anti-human CD68 (BioLegend). After incubation for 30 min at room temperature in darkness, cells were washed again before analysis. After rinsing, all cells were resuspended in the same buffer for flow analysis in the Accuri C6 Flow Cytometer®.

Detection of In Vivo CXCR7 in Plaque Macrophages of ApoE-null Mice—*ApoE*-deficient mice and genetically matched C57BL/6 normal control mice (Jackson Laboratory) with same ages and genders were employed in this study as we previously described.(13) Mice were fed standard chow diet with 4.5% fat (PMI Feeds, St. Louis, MO). All mice were maintained in a facility free of well-defined pathogens under the supervision of the Biological Resource Unit at Auburn University. All animal protocols were approved by Auburn Institutional Animal Care and Use Committee; and the investigation conforms to the Guide for the Care and Use of Laboratory Animals published by the United States National Institutes of Health.

We fed mice with normal chow diet for 16 weeks and then evaluated atherosclerotic lesions in aortic sinus by oil red O staining as reported previously.(13) The mouse hearts and aorta were perfused, dissected, and subjected to determination of atherosclerosis, as previously described (13). Briefly, mice requiring aortic tissue analysis were euthanized by deep anesthesia with ketamine/xylaxine (170 mg/kg and 5 mg/kg, respectively, peritoneal injection once) prior to intracardiac perfusion with 4% paraformaldehyde in PBS. The hearts were embedded in optimal cutting temperature (OCT) medium and frozen, after which serial sections (10 μm) were taken from the aortic sinus. Images were obtained of the sections following staining with oil red O (counterstaining with H&E). The CXCR7-positive and F4/80-positive areas were determined in 4 sections from each mouse, using 80-μm intervals between the sections; the results were confirmed in three *ApoE*-null and control mice.

Immunohistochemistry Analysis—Mouse aortic sections were fixed in cold methanol for 10 min and rinsed twice in PBS. Sections were blocked with 5% horse serum at room temperature for 1 h. The anti-F4/80 or sheep anti-mouse CXCR7 antibody (R&D Systems, Catalogue number: AF4227) or isotype control Abs were added to the sections at 10 μg/ml and incubated at room temperature for 1.5 h. Sections were rinsed thoroughly in PBS and incubated with Dylight 488-conjugated anti-rat IgG or NL637-conjugated donkey anti-sheep IgG (R&D Systems) for 45 min. Sections were then counterstained with H&E and oil red O, rinsed thoroughly in PBS and cover slipped with Vectashield Mounting Medium (Vector laboratories), as previously reported. (13) All images were acquired and captured on an AMG EVOS® digital inverted multi-functional microscope.

Silencing of CXCR7 and CXCR4 Receptors by siRNA—To knockdown the CXCR7 and CXCR4 receptors, THP-1 cells were transfected with the four sequence SMART pools (ON-TARGET plus CXCR7 siRNA: L-013212−00−0005; ON-TARGET plus CXCR4 siRNA: L-005139-00-0005; or ON-TARGET plus Non-targeting scramble control siRNA: D-001810-10^{-05}, Dharmacon) by electroporation using the Lonza Nucleofector technology (4D-Nucleofector®). We followed an optimized protocol reported recently by Schnoor *et al.* (36) Briefly, a human Monocyte Nucleofector Kit (Lonza) was used for the transfection and the number of THP-1 cells was 2.5×10^6 per transfection cuvette. THP-1 cells were recovered 4 h after transfection in Human Monocyte Nucleofector Medium (Lonza) supplemented with 20% FBS. Transfected cells per cuvette were transferred into single well of 6-well plates containing 1.5 ml fresh Human Monocyte Nucleofector Medium supplemented as described above and containing PMA 40 nM or "IFN-γ (100 ng/ml) + LPS (1 μg/ml)" for macrophage differentiation for 24∼48 h. Real-time RT-PCR assay and Western blotting were performed to confirm the decrease or suppression of CXCR7/4 mRNA and protein expression respectively after 24∼48 h post-transfection. For cell stimulation, transfected and differentiating cells were starved at least for 8 h before stimulated by SDF-1, I-TAC, or TC14012 for the indicated times.

Macrophage Phagocytosis and Acetylated LDL Uptake—Macrophage phagocytic activity was measured using the Vybrant Phagocytosis Assay Kit (Invitrogen) and Dil-ac-LDL uptake assay (Invitrogen). Briefly, human monocytes were differentiated into macrophages in 96-well plate by incubation with "100 ng/ml IFNγ + 1 μg/ml LPS" for 48 h, after which cells were starved for 10 h. The cells in four replicates were stimulated with agonists for 2 h with or without pre-treatment with inhibitors. The cells were further incubated with heat-inactivated, fluorescein-labeled *Escherichia coli* K-12 BioParticles for 2 h, after which extracellular fluorescence was quenched by trypan blue and phagocytic activity was quantified by measuring fluorescence intensity of the uptaken particles emission at 520 nm with an excitation at 485 nm using a microplate reader (FLUOstar). To determine cellular uptake of acetylated-LDL, the same experimental procedure for *E. coli* phagocytosis was used as described above with the following modifications: 1) fluorescein-labeled *E. coli* K-12 BioParticles were replaced by Dil-ac-LDL (10 μg/ml); 2) trypan blue quenching was replaced by three times PBS washing; and 3) the red fluorescence intensity was determined in the Varioskan Flash Multimode Plate Reader (fluorescence Ex/Em: 554/571). The negative controls were prepared by adding vehicles and fluorescence labeled

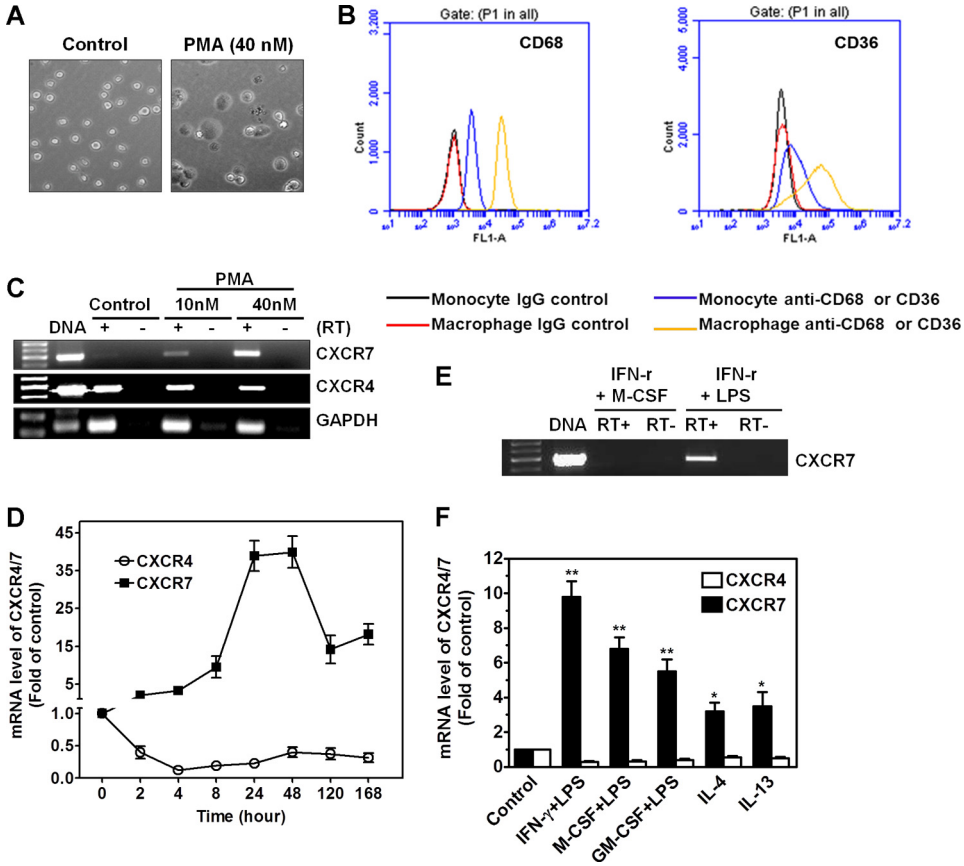

FIGURE 1. **Induction of CXCR7 mRNA during monocyte-to-macrophage differentiation.** *A*, treatment of THP-1 cells (floating cells) with 40 nM PMA for 48 h induced monocyte differentiation with morphological changes into macrophage-like cells (adherent cells). Images magnification: ×20. *B*, THP-1 monocytes and PMA-driven THP-1 macrophages were stained with CD68 or CD36 antibodies and the respective isotype-matched IgG controls before analyzed by a standard flow cytometry assay. Monocytes and macrophages were identified and gated by their forward and side scatter characteristics. Flow cytometry plots are representative results from three independent experiments showing fluorescence intensity of isotype control antibodies (*black* or *red line*) compared with the CD68- or CD36-selective antibodies (*blue* or *yellow line*). *C*, mRNA expression of CXCR4 and CXCR7 in vehicle-treated cells (control), and in cells treated with 10 nM or 40 nM PMA for 48 h. RT-PCR performed without reverse transcriptase (RT-) and genomic DNA was used as negative controls and positive controls, respectively ($n = 3$). *D*, kinetics of CXCR4 and CXCR7 mRNA expression during monocyte-to-macrophage differentiation induced by 40 nM PMA for the indicated time periods. The mRNA levels were determined by real-time PCR and presented as relative fold changes compared with control cells after normalized to GAPDH ($n = 5$). *E*, CXCR7 mRNA was induced in THP-1 macrophages polarized by IFN-γ (100 ng/ml) and LPS (1 μg/ml), but not by IFN-γ (100 ng/ml) and M-CSF (10 ng/ml). *F*, change of CXCR4/7 mRNA expression in human primary monocytes after differentiation into macrophages by indicated reagents for 48 h ($n = 5$), *, $p < 0.05$; **, $p < 0.01$.

probes without cells; and macrophages without stimulation were used as positive controls. Results were expressed as the percentage of increase compared with positive controls after deduction of negative controls as suggested by the kit instructions.

Materials—Recombinant human SDF-1a, I-TAC, M-CSF, GM-CSF, TNFα, IL-4, IL13, and IFN-γ were purchased from R&D System. AMD3100 was obtained from EMD chemicals, TC14012 and PMA from Tocris Bioscience. The CXCR3-selective antagonist Compound 6c was purchased from Axon Medchem. DNA primers were purchased from Integrated DNA Technologies, and LPS from Sigma.

Data Analysis—Data are expressed as the mean ± S.E. The means of two groups were compared using Student's *t* test (unpaired, two tailed), and one-way analysis of variance was used for comparison of more than 2 groups with $p < 0.05$ considered to be statistically significant. Unless otherwise indicated, all experiments were repeated at least three times.

RESULTS

CXCR7 mRNA Is Induced during Monocyte-to-Macrophage Differentiation—To investigate whether CXCR7 is induced during monocyte-to-macrophage differentiation, THP-1 cells were treated with PMA, a well-established macrophage inducer. As expected, THP-1 cells acquired a macrophage-like morphology after stimulation by PMA (40 nM) for 48 h (Fig. 1*A*). Macrophage differentiation was confirmed by up-regulated CD68 and CD36 (Fig. 1*B*). RT-PCR analysis showed that undifferentiated THP-1 cells expressed high level of CXCR4, but not CXCR7 mRNA; however, PMA treatment induced CXCR7 mRNA expression, with a simultaneous down-regulation of CXCR4 mRNA (Fig. 1*C*). Real-time PCR assay confirmed that CXCR7 mRNA was induced as early as 2 h in response to PMA, reached maximal level at 24~48 h, and then declined to a level still significantly higher than that of time-controlled undifferentiated cells (Fig. 1*D*). In contrast, the same differentiation protocol suppressed CXCR4 mRNA expression more than 50% in the observation window (Fig. 1*D*).

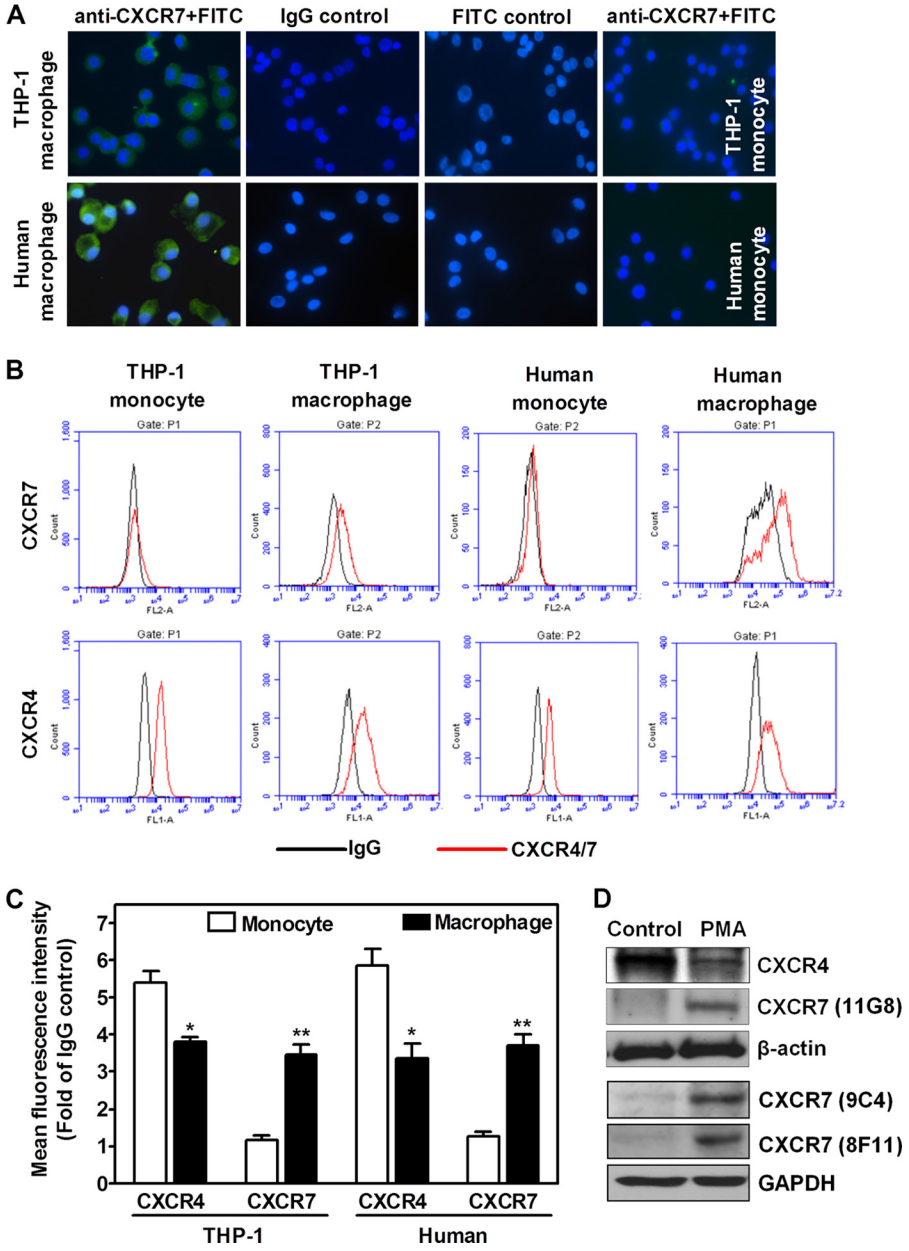

FIGURE 2. **Detection of CXCR4/7 antigens on monocytes *versus* macrophages.** *A*, immunofluorescent detection of CXCR7 (*green*) on macrophages differentiated by IFN-γ (100 ng/ml) and LPS (1 μg/ml) from human primary monocytes (human macrophage). Nuclei were shown by DAPI staining (*blue*). Representative images from three healthy blood donors were shown. Macrophages differentiated from PMA-driven THP-1 cells were used as positive controls. Isotype-matched first antibodies (IgG) and FITC-conjugated secondary antibodies were used for negative controls. CXCR7 was not detected in THP-1 monocytes and primary monocytes (human monocyte). Original magnification: ×60. *B*, THP-1 monocytes, PMA-driven THP-1 macrophages, primary monocytes, and their differentiated macrophages (100 ng/ml IFN-γ+1 μg/ml LPS) were stained with CXCR4 or CXCR7 antibodies and the respective isotype-matched IgG controls before analyzed by flow cytometry. Flow cytometry plots are representative results from three independent experiments showing fluorescence intensity of isotype control antibodies (*black line*) compared with the CXCR4- or CXCR7-selective antibodies (*red line*). *C*, summarized quantitative data for *panel B*. *, $p < 0.05$; **, $p < 0.01$. *D*, CXCR4 and CXCR7 protein levels were determined by Western blotting in total cell lysates isolated from vehicle-treated control monocytes and PMA-differentiated macrophages. Similar data were obtained in three independent experiments.

To determine whether CXCR7 up-regulation in THP-1 cells is limited to the reagent PMA, we treated the cells with alternative differentiation factors that are more pathologically relevant. Fig. 1*E* shows that CXCR7 mRNA was similarly induced in response to IFN-γ+LPS, but not to IFN-γ+M-CSF. A similar pattern of CXCR4/7 mRNA expression change was observed in human primary monocytes when they were differentiated into M1 and M2 macrophages with a more robust induction of CXCR7 mRNA in M1 cells than in M2 cells (Fig. 1*F*).

CXCR7 Protein Expression in Monocytes versus Macrophages—Immunofluorescent assay showed that CXCR7 protein was expressed in macrophages differentiated from primary monocytes after 48 h treatment with IFN-γ+LPS, but it was not detected in primary human monocytes (Fig. 2*A*). Of notes, no positive staining was observed once CXCR7 monoclonal antibody was replaced by its IgG control antibody or when only FITC-conjugated secondary antibody was used (Fig. 2*A*).

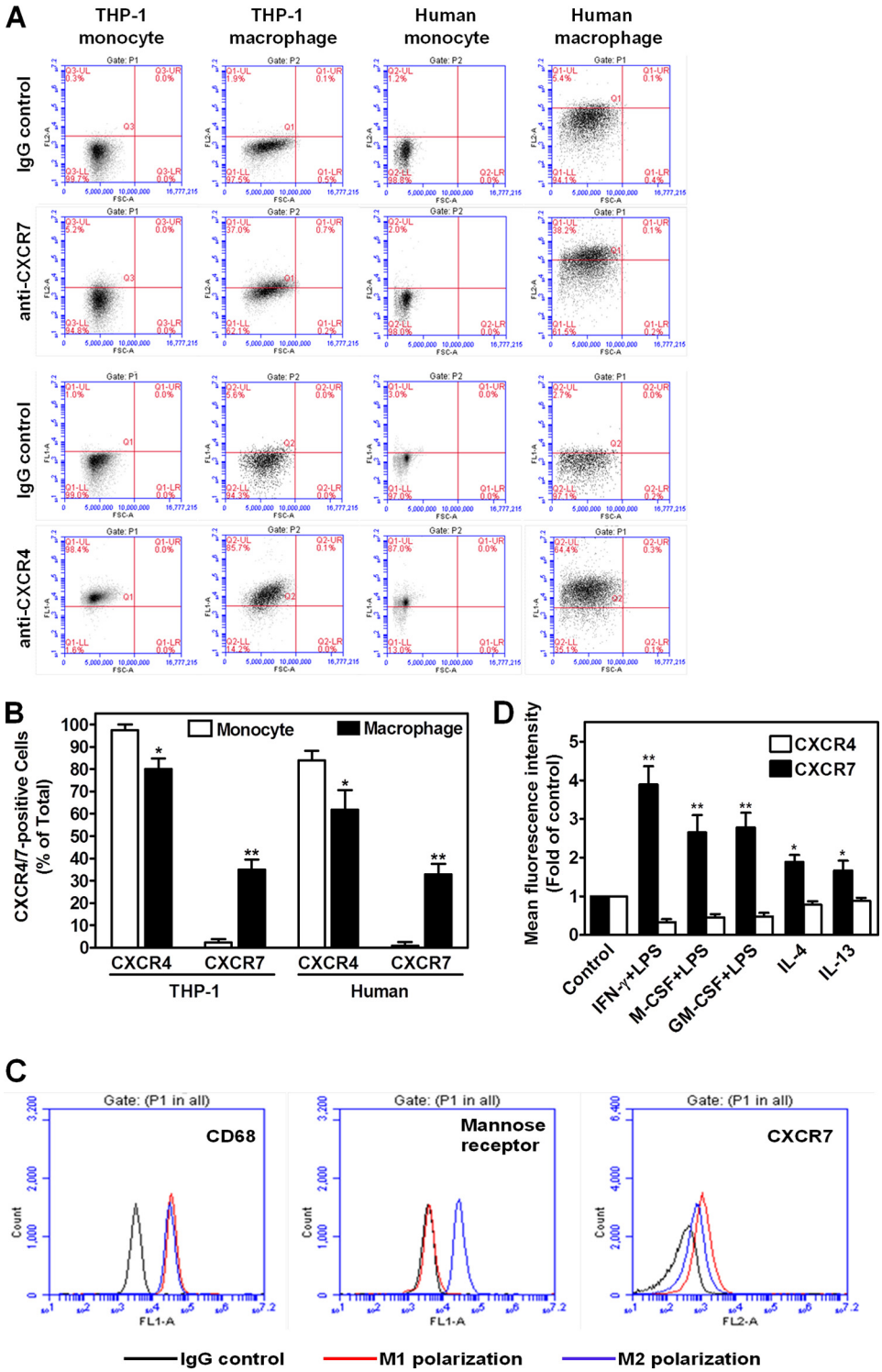

FIGURE 3. **Differential expression of CXCR4/7 on monocytes and macrophages with different phenotypes.** *A*, detection of CXCR4- or CXCR7-positive cells in monocytes *versus* macrophages. THP-1 monocytes, PMA-driven THP-1 macrophages, primary monocytes and their differentiated macrophages (100 ng/ml IFN-γ+1 μg/ml LPS) were stained with CXCR4 or CXCR7 antibodies and their respective isotype-matched IgG controls before analyzed by flow cytometry assays. Flow cytometry plots are representative results from three independent experiments. *B*, summarized quantitative data for *panel A*. *, $p < 0.05$; **, $p < 0.01$. *C*, CXCR7 expression in M1 *versus* M2 macrophages. Human primary monocytes were differentiated into M1 or M2 phenotype by IFN-γ+LPS (M1) or IL-4(M2), respectively for 48 h. Then, the cells were stained with CD68, CD206(mannose receptor) or CXCR7 antibodies and the respective isotype-matched IgG controls before analyzed by a standard flow cytometry assay. Macrophages were identified and gated by their forward and side scatter characteristics. Flow cytometry plots are representative results from three independent experiments showing fluorescence intensity of isotype control antibodies (*black line*) compared with the CD68, CD206, or CXCR7-selective antibodies (*blue or red line*). *D*, differential change of cell surface CXCR4 *versus* CXCR7 during monocyte-to-macrophage differentiation. Cell surface CXCR4 or CXCR7 antigen levels were determined by flow cytometry assays after the human primary monocytes were differentiated into macrophages by indicated reagents for 48 h. Mean fluorescence intensity for CXCR4 or CXCR7 antigen was determined after normalization with respective IgG controls. ($n = 5$), *, $p < 0.05$; **, $p < 0.01$.

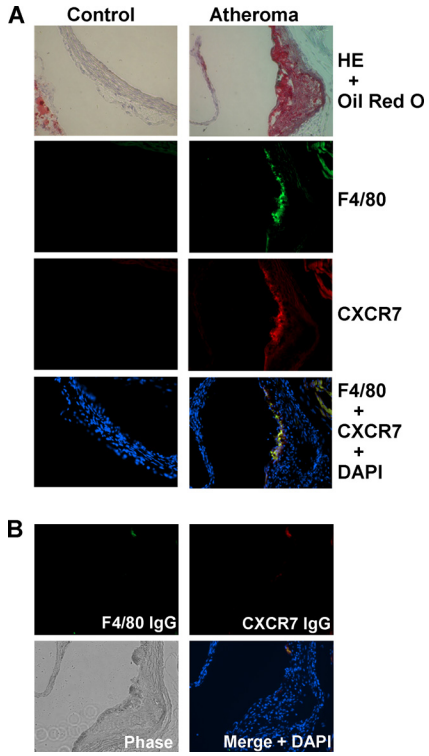

FIGURE 4. **Detection of CXCR7 in macrophage-positive area of aortic atheroma in *ApoE*-null mice.** *A*, atherosclerotic plaque was revealed by oil red O staining with H&E counterstain on aortic sinus sections from 16-week old female *ApoE*-null mice, but not from age-matched female control C57BL/6 mice (*top*). Immunofluorescent detection of macrophage marker F4/80 (*green*), CXCR7 (*red*), and their co-localization in atheroma. Nuclei were shown by DAPI staining (*blue*, *bottom*). Representative images from three mice in each group were shown (original magnification: ×20). *B*, specificity of fluorescence-conjugated antibodies was confirmed on sections stained negative with control IgG for F4/80 and CXCR7. The morphology of sections was revealed by a phase-contrast mode.

To confirm whether CXCR7 is expressed on cell surface, we performed flow cytometry assays. Fig. 2, *B* & *C* show that CXCR7 was not expressed in THP-1 cells or in primary monocytes; however, upon differentiation by IFN-γ+LPS for 48 h, cell surface CXCR7 antigen was significantly increased in THP-1 macrophages or in macrophages differentiated from primary cells. In contrast, cell surface CXCR4 antigen decreased during this differentiation process as measured by mean fluorescence intensity (Fig. 2*C*). We found a similar change when the percentages of CXCR4-positive or CXCR7-positive cells were determined (Fig. 3, *A* & *B*). In addition, we observed that M1 polarization of primary macrophages exhibited more CXCR7 antigen than did M2 polarization (Fig. 3, *C* & *D*). Our Western blotting assay further showed that during monocyte-to-macrophage differentiation, CXCR7 total protein was detected by three different specific mouse monoclonal antibodies, (15) whereas CXCR4 protein level was down-regulated (Fig. 2*D*).

In Vivo Expression of CXCR7 in Atherosclerotic Plaques of ApoE-null Mice—To assess the *in vivo* relevance of our finding, we extended our observation to *ApoE*-null mice with atherosclerotic lesions. Immunofluorescent analysis on serial sections of mouse aorta from *ApoE*-null mice showed that CXCR7 protein was expressed in the atherosclerotic lesions (Fig. 4*A*). In addition, CXCR7 protein expression was co-localized with F4/80-positive macrophage areas of the atheroma defined by oil red O staining (Fig. 4*A*). In contrast, the same parallel analysis did not detect any noticeable CXCR7 protein in the sex- and age-controlled C57BL6/J mice, which were F4/80-negative in the aorta sections (Fig. 4*A*). Fig. 4*B* shows that the control IgG for either F4/80 or CXCR7 did not exhibit significant staining, indicating the specificity of the assay system.

Role of CXCR7 in SDF-1 Signaling during Monocyte-to-Macrophage Differentiation—To determine whether CXCR7 plays a role in SDF-1 signaling, we first compared SDF-1 signaling profiles in human primary monocytes *versus* macrophages. As shown in Fig. 5, *A* & *B*, stimulation of either THP-1 cells or human primary monocytes with SDF-1 dose-dependently activated the ERK and AKT pathways, with negligible or no effects on the p38 and JNK pathways. However, once the cells were differentiated into macrophages by IFN-γ+LPS, the ERK and AKT pathways were not activated by SDF-1 (Fig. 5*C*&D). Interestingly, on these macrophages, SDF-1 became a strong activator of the p38 and JNK pathways, in a level comparable to a maximal dose of LPS (Fig. 5 *C* & *D*). This stimulation was time-dependent with a maximal effect at 15 min (data not shown). These data suggest that CXCR7 induction may switch SDF-1 signaling from pro-survival ERK and AKT to pro-inflammatory JNK and p38 pathways during monocyte-to-macrophage differentiation.

To further evaluate the role of CXCR7 in SDF-1 signaling in macrophages, we stimulated the cells with the CXCR7-selective peptide agonist TC14012 (16). Fig. 6, *A* & *B* show that TC14012 activated p38 and JNK pathways in a dose- and time-dependent manner, with a slight inhibition on the ERK and AKT pathways, suggesting a potential role of CXCR7 in SDF-1 signaling in macrophages.

To verify the contribution of CXCR7, we silenced *CXCR7* gene in THP-1 cells using siRNA techniques. Fig. 6, *C* & *D* show that CXCR7 mRNA and protein expression were significantly suppressed by transfection of *CXCR7*-selective siRNAs, but not by scramble control siRNAs. Of note, transfection of *CXCR7*-selective siRNA did not affect CXCR4 expression (Fig. 6*D*). In addition, silencing CXCR7 abolished the effect of SDF-1 and TC14012 on p38 and JNK activation in these macrophages, with no impact on LPS signaling (Fig. 6*E*). Furthermore, the ERK and AKT pathways were not changed in response to SDF-1, TC14012 or LPS after silencing CXCR7 (Fig. 6*E*).

To further assess the contribution of CXCR4 in SDF-1 signaling in macrophages, we knocked down CXCR4 by siRNA. Fig. 6*F* shows that CXCR4-selective siRNA suppressed CXCR4, but not CXCR7 or GAPDH protein expressions. In addition, SDF-1- or TC14012-induced p38 and JNK activations were not affected by silencing of CXCR4 (Fig. 6*G*), indicating CXCR7 signaling is independent of CXCR4 in macrophages.

Role of CXCR7 in Macrophage Phagocytosis and Uptake of Acetylated LDL—Next, we evaluated whether CXCR7 plays a role in macrophage functions. We focused on phagocytosis, the primary function of macrophages. Fig. 7*A* shows that stimulation of macrophages by either SDF-1 or TC14012 significantly increased cellular phagocytosis as evidenced by increased uptake of FITC-labeled *E. coli*. Of note, we observed that

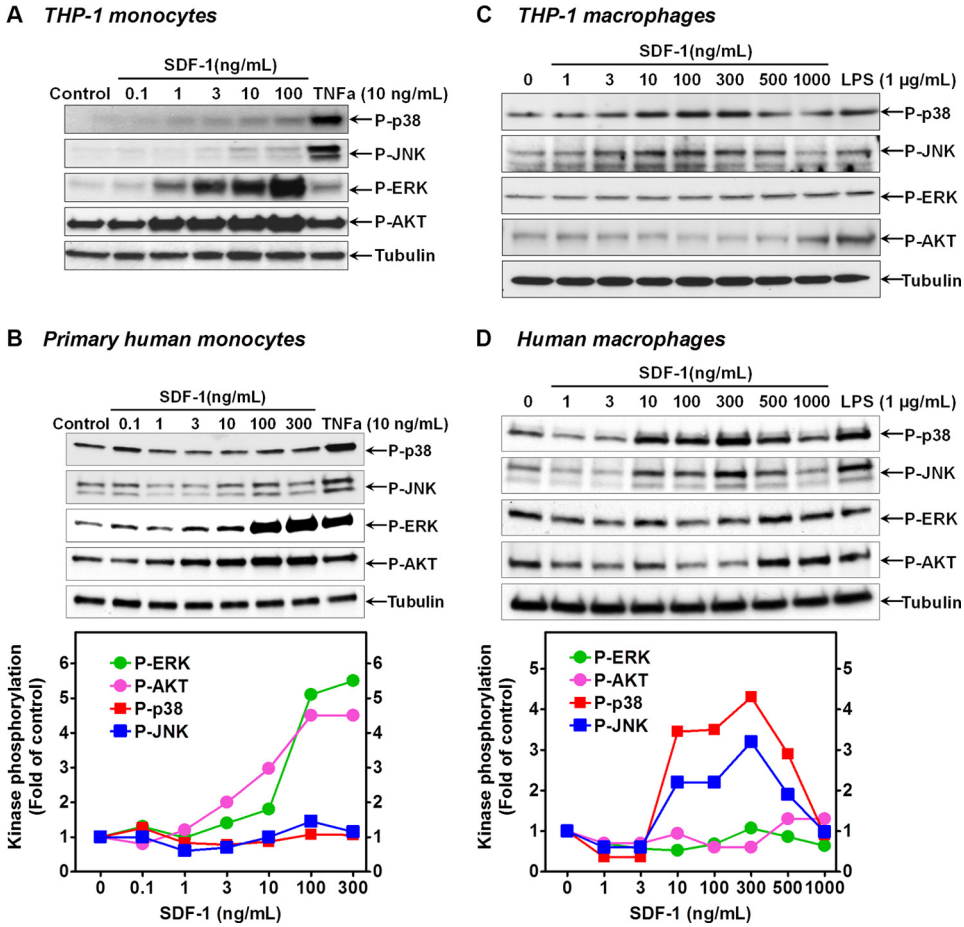

FIGURE 5. **Differential SDF-1 signaling in monocytes *versus* macrophages.** *A*, cellular phosphorylation levels of p38, JNK, ERK, and AKT in THP-1 monocytes were determined by Western blotting after the cells were stimulated by SDF-1 or TNFα for 15 min at the indicated concentrations. *B*, similar data were obtained in primary human monocytes. Dose-dependent effect of SDF-1 on the phosphorylation of p38, JNK, ERK, and AKT in THP-1 macrophages (*C*) and human primary macrophages (*D*) as determined by Western blotting after the cells were stimulated by SDF-1 or LPS for 15 min at the indicated concentrations. The mean densitometric analysis of three separate experiments is normalized to respective total kinase loading controls (not shown) and the summarized data were shown in the bottom graphs. For clarity, only tubulin loading controls were shown; and the error bars with markers for the statistical significance have been omitted.

TC14012 was more efficacious than SDF-1, and both are more efficacious than IFN-γ (Fig. 7*A*). In addition, treatment of the cells with CXCR4-selective antagonist AMD3100 had no inhibition on SDF-1's effect (data not shown). In contrast, siRNA silencing of CXCR7 almost eliminated the effect of either SDF-1 or TC14012, but not that of IFN-γ (Fig. 7*B*), suggesting a role for CXCR7 in macrophage phagocytosis.

To explore the role of JNK and p38 in CXCR7-mediated cellular phagocytosis, well established selective inhibitors for p38 and JNK were employed. Fig. 7*C* shows that inhibition of either JNK or p38 significantly suppressed SDF-1- or TC14012-induced cellular phagocytosis. Together, these data suggest that SDF-1 promotes macrophage phagocytosis via CXCR7-mediated JNK and p38 pathways.

We further extended the study to a more atherosclerosis relevant context. Fig. 7*D* shows that SDF-1 and TC14012 increased macrophage uptake of Dil-ac-LDL, and the efficacy of SDF-1 was comparable to that of IgG, activator of Fcγ receptors. In addition, we confirmed that this effect was mediated by CXCR7-induced activation of JNK and p38 pathways (Fig. 7, *E* & *F*), and that it was not affected by CXCR4 blockage (data not shown).

Role of CXCR7 in I-TAC-induced Macrophage Signaling and Phagocytosis—Since I-TAC is the other endogenous agonist for CXCR7, we evaluated whether the I-TAC/CXCR7 pathway has the same role as SDF-1 did. Fig. 8*A* shows that neither monocytes nor macrophages express detectable level of cell surface CXCR3, another receptor for I-TAC, but it is highly expressed in blood lymphocytes. Consistent with this, stimulation of monocytes by I-TAC did not induce any effect on the ERK, AKT, p-38 and JNK pathways, but SDF-1 strongly activated ERK and AKT as expected (Fig. 8*B*). However, I-TAC significantly activated p38 and JNK in macrophages in a time-dependent manner, albeit not as efficacious as SDF-1 (Fig. 8*C*). Of note, like SDF-1, I-TAC had no effect on the ERK and AKT pathways in macrophages. Fig. 8*D* shows that pretreatment of macrophages with the compound 6c, a CXCR3-selective antagonist, had no impact on I-TAC-induced p38 and JNK activation. In contrast, CXCR7 silencing by siRNA almost abolished the effect of I-TAC on p38 and JNK in macrophages (Fig. 8*E*), indicating a role for CXCR7 in I-TAC signaling.

Finally, we verified whether I-TAC promotes macrophage phagocytosis through CXCR7. Fig. 9, *A*–*C* shows that stimulation of macrophages with I-TAC increased macrophage uptake

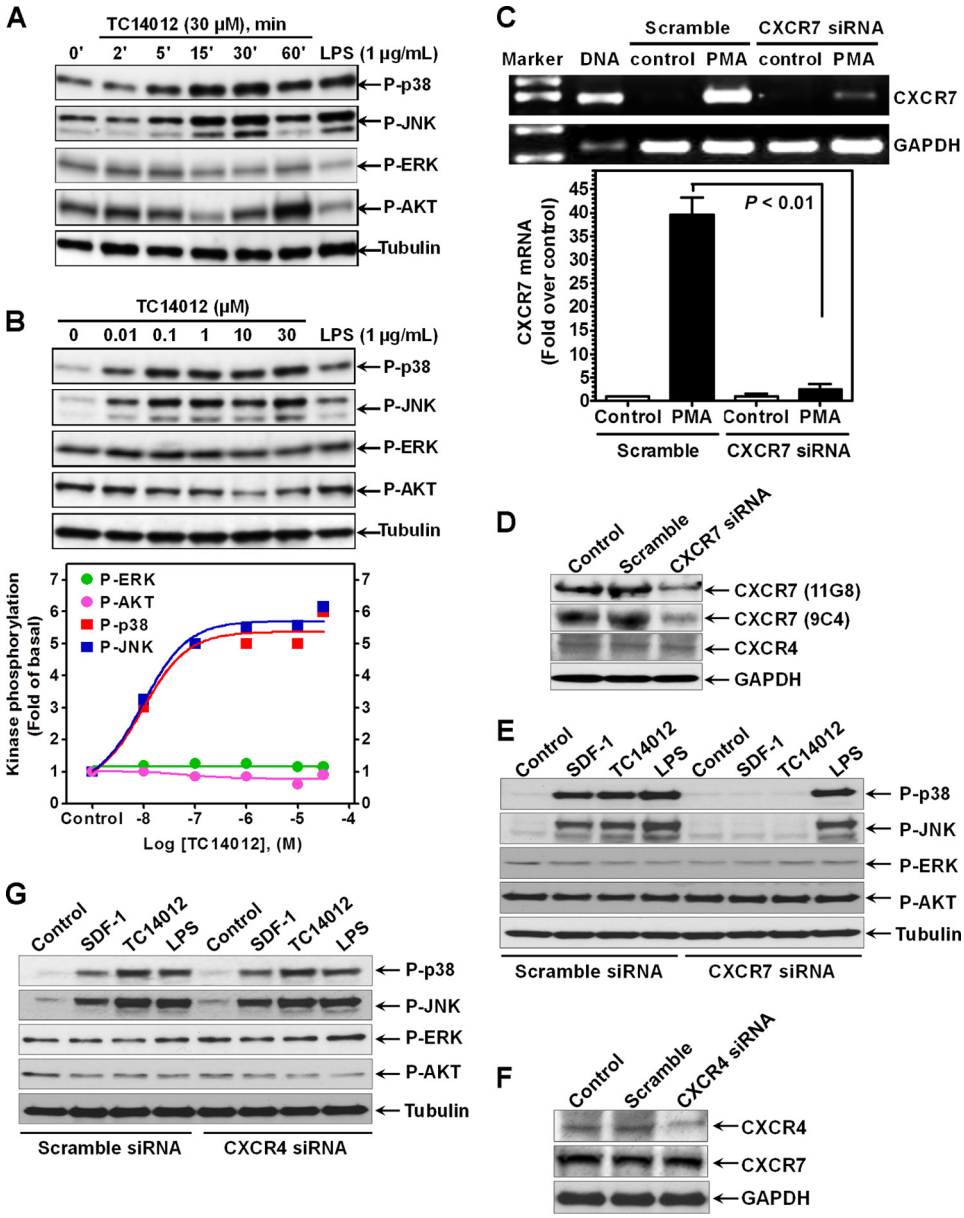

FIGURE 6. **Evidence of CXCR7 signaling in macrophages.** *A*, cellular phosphorylation levels of p38, JNK, ERK, and AKT in macrophages differentiated from human primary monocytes (100 ng/ml IFN-γ + 1 μg/ml LPS for 48 h) were determined by Western blotting after the cells were stimulated by TC14012 or LPS (15 min) for the indicated concentrations and times. *B*, dose-dependent effect of TC14012 on the phosphorylation of p38, JNK, ERK, and AKT in macrophages as determined by Western blotting after the cells were stimulated by TC14012 or LPS for 15 min at the indicated concentrations. The mean densitometric analysis of three separate experiments is normalized to respective total kinase loading controls (not shown), and the summarized data were shown in the bottom graph. *C*, real-time PCR analysis of CXCR7 mRNA expression after the THP-1 cells were nucleofected with CXCR7 siRNA or scramble siRNA with or without (control) further PMA-induced macrophage differentiation (48 h), $n = 4$. *D*, knockdown of CXCR7 protein expression was confirmed by Western blotting using two different antibodies (11G8 and 9C4). CXCR7 siRNA had no effect on CXCR4 and GAPDH expression. *E*, impact of CXCR7 knockdown by siRNA on SDF-1- and TC14012-induced effect on p38, JNK, ERK and AKT pathways in THP-1 macrophages. Scramble siRNA and LPS serve as respective controls. *F*, CXCR4-selective siRNA suppressed CXCR4, but not CXCR7 and GAPDH protein expression. *G*, no impact of CXCR4 knockdown by siRNA on SDF-1- and TC14012-induced effect on p38, JNK, ERK, and AKT pathways in THP-1 macrophages. Blots are representative data from three independent experiments showing similar results.

of *E. coli* particles, which was suppressed by siRNA silencing of CXCR7 or blocking the p38/JNK pathways, but not by CXCR3 blockade. Similarly, we found that I-TAC increased macrophage uptake of Dil-ac-LDL in a CXCR7 and p38/JNK-dependent but CXCR3-independent mechanism (Fig. 9, *D–F*).

DISCUSSION

Here we show for the first time that CXCR7 is induced during monocyte-to-macrophage differentiation and that CXCR7 is expressed in macrophage-positive areas of mouse aortic atheroma. Furthermore, we have demonstrated that CXCR7 is required for SDF-1 activation of the JNK and p38 pathways in macrophages, leading to enhanced cellular phagocytosis.

The role of SDF-1 in the biology of leukocytes and stem/progenitor cells has been extensively investigated. It has been established that SDF-1 is one of the most efficacious chemoattractant for multiple leukocytes, including monocytes (8). For a while, it was thought that CXCR4 is the only receptor that

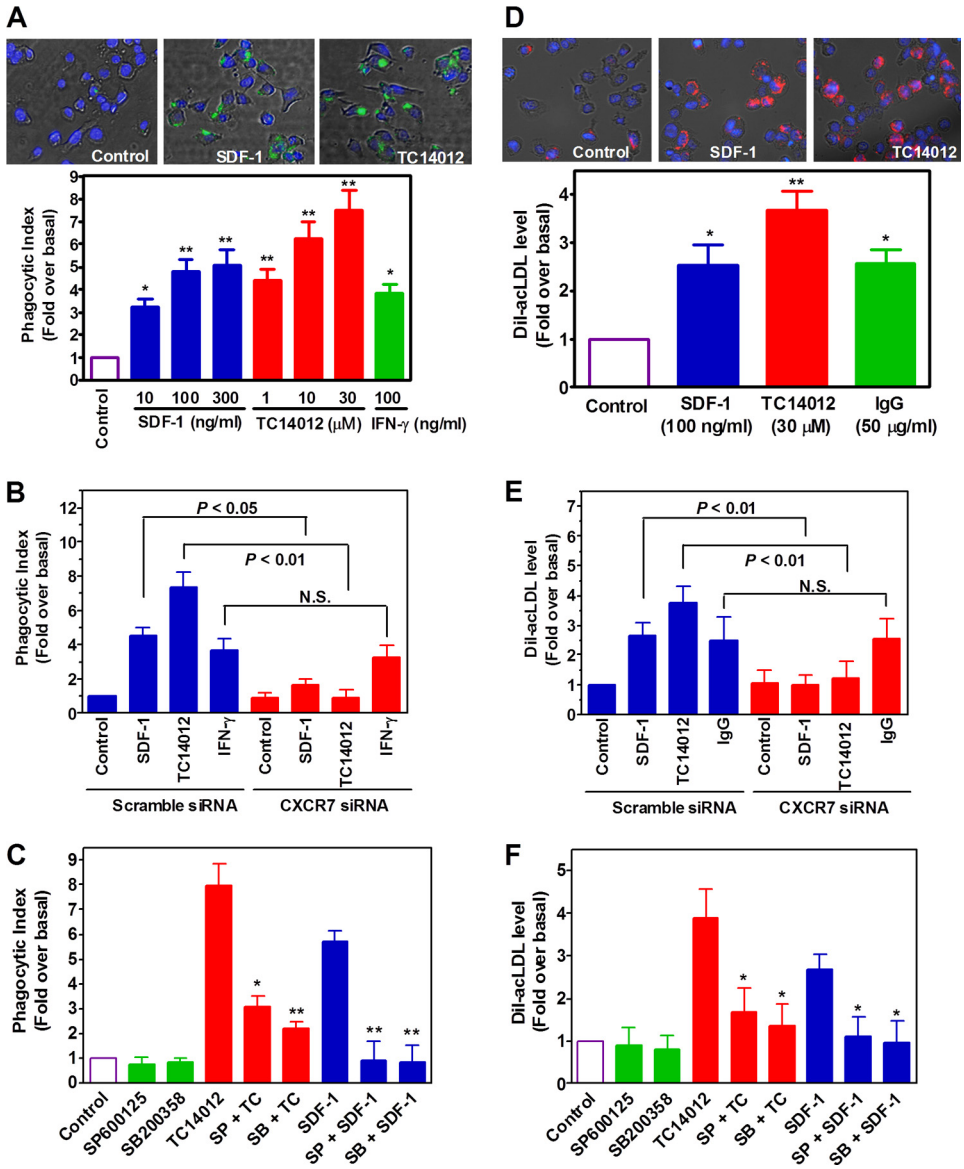

FIGURE 7. **Role of CXCR7 in the phagocytic activity of macrophages.** *A*, macrophages differentiated from THP-1 monocytes were starved and activated by vehicle (control), SDF-1, TC14012 or IFN-γ for 2 h, after which FITC-labeled *E. coli* were added and further incubated for 2 h. Then phagocytic index was determined by measuring green fluorescence intensity emitted by the uptaken particles. Shown are merged images of macrophages (phase contrast) with internalized FITC-*E. coli* particles (*green*) and DAPI-positive nuclei (*blue*). Images magnification: ×20, *, $p < 0.05$, ** $p < 0.01$ compared with the control, $n = 5$. *B*, effect of CXCR7 knockdown by siRNA on 300 ng/ml SDF-1- and 30 μM TC14012-induced phagocytic activities in macrophages. *N.S.* stands for statistic non-significance. $n = 5$. *C*, after pretreating the cells with or without SP600125 (30 μM) or SB200358 (10 μM) for 40 min, cells were stimulated by TC14012 (30 μM) or SDF-1 (300 ng/ml) for 2 h. Then phagocytosis assay was performed as described above. *, $p < 0.05$; **, $p < 0.01$ compared with the corresponding controls, $n = 6$. *D*, effect of SDF-1, TC14012, and IgG (FcγR agonist) on the uptake of Dil-acLDL in THP-1 macrophages, $n = 5$. *E*, effect of CXCR7 knockdown by siRNA on 300 ng/ml SDF-1- and 30 μM TC14012-induced uptake of Dil-acLDL in macrophages. *N.S.* stands for statistic non-significance, $n = 5$. *F*, after pretreating the cells with or without SP600125 (30 μM) or SB200358 (10 μM) for 40 min, cells were stimulated by TC14012 (30 μM) or SDF-1 (300 ng/ml) for 2 h. Then Dil-acLDL uptake was measured as described in "Experimental Procedures." *, $p < 0.05$ compared with the controls, $n = 5$.

mediates various functions of SDF-1. This concept was supported by the fact that genetic knock-out of the *CXCR4* gene recaptured the lethal phenotype initially observed in *SDF-1*-deficent mice.(11) This knowledge led to the development of the FDA-approved drug plerixafor (17), which is currently used for efficient mobilization of bone marrow stem cells.(18) However, Balabanian *et al.* recently showed that the orphan RDC1 receptor binds to SDF-1 with an even higher affinity than CXCR4 (19). Few follow-up studies generate conflicting data regarding CXCR7 expression in leukocytes (20, 21). A recent, more sophisticated study convincingly demonstrated that normal peripheral blood leukocytes in humans or mice do not express CXCR7, and further pointed out that the conflicting earlier observations were due to nonspecific staining of polyclonal CXCR7 antibodies (12, 15). In the present study, by using three specific CXCR7 monoclonal antibodies, we confirmed by multiple approaches that the monocytic THP-1 cells and human primary monocytes do not express CXCR7. This is supported by our RT-PCR analysis which shows no significant CXCR7 mRNA expression in these monocytes. However, we found unexpectedly that CXCR7 is induced during monocyte-to-macrophage differentiation. This notion is supported by

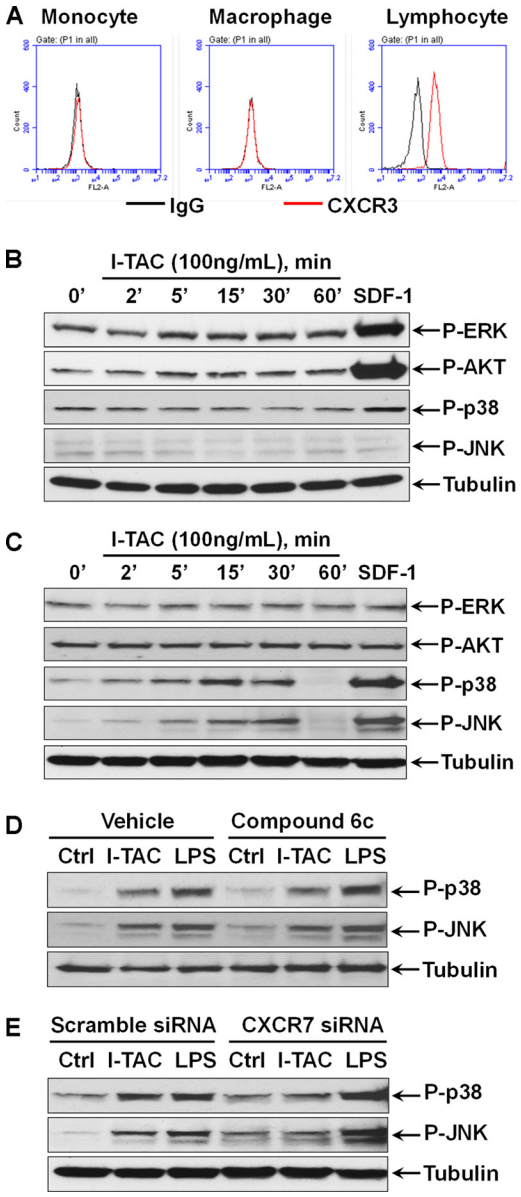

FIGURE 8. **Role of CXCR7 in I-TAC signaling in monocytes *versus* macrophages.** *A*, THP-1 monocytes, PMA-driven THP-1 macrophages, and human blood lymphocytes were stained with CXCR3 antibody and the isotype-matched IgG control before being analyzed by flow cytometry. Flow cytometry plots are representative results from three independent experiments showing fluorescence intensity of isotype control antibody (*black line*) compared with the CXCR3-selective antibody (*red line*). *B*, cellular phosphorylation levels of ERK, AKT, p38, and JNK in THP-1 monocytes were determined by Western blotting after the cells were stimulated by I-TAC for the indicated times. SDF-1 (100 ng/ml) stimulation for 15 min as a positive control. *C*, time-dependent effect of I-TAC on the phosphorylation of ERK, AKT, p38, and JNK in THP-1 macrophages. SDF-1 (100 ng/ml) stimulation for 15 min as a positive control. *D*, no effect of CXCR3-selective antagonist compound 6c (10 μM) on I-TAC (100 ng/ml)-induced p38 and JNK activation. *E*, effect of CXCR7-selective siRNA on I-TAC (100 ng/ml)- and LPS (1 μg/ml)-induced activation of p38 and JNK. For clarity, only tubulin loading controls are shown. Blots are representative data from three independent experiments showing similar results.

several lines of evidence: 1) PMA treatment of THP-1 cells induced up-regulation of CXCR7 mRNA along with cell differentiation into macrophage-like morphology and expression of macrophage markers; 2) CXCR7 induction is not limited to the pharmacological reagent PMA, and indeed can be mimicked by IFN-γ+LPS, pathological activators of monocytes and macrophages; 3) We confirmed by Western blotting and immunofluorescent assays that CXCR7 mRNA induction is accompanied by CXCR7 protein up-regulation; 4) we verified by flow cytometry that monocyte surface has no or negligible amount of CXCR7 antigen, and once differentiated into macrophages, their cell surface CXCR7 antigen is up-regulated; and 5) we found more CXCR7 induction in M1 macrophages than M2 cells. Thus, we have provided compelling evidence indicating that during monocyte-to-macrophage differentiation, CXCR7 is induced at mRNA, total protein and cell surface levels. Our finding reinforces the idea that CXCR7 induction may be a more broadly related phenomenon for terminal cell differentiation, since a prior study found that CXCR7 is induced during B cell maturations (21).

Although CXCR4 is not the focus of this study, we consistently observed that this SDF-1 receptor was down-regulated during macrophage differentiation. This result indicates that the two SDF-1 receptors exhibit dynamic regulation in opposite directions during monocyte-to-macrophage differentiation. Prior study found that isolated monocytes showed decreased responsiveness to SDF-1 through unknown mechanism (22). Our finding suggests that this could be attributed to decreased CXCR4 expression and/or CXCR7 induction. We and others reported that plasma level of SDF-1 in normal mice or humans is around 3.5 ng/ml (6, 13), which based on this study is high enough to achieve a steady-state activation of cell signaling pathways such as ERK and AKT. This finding suggests that in normal physiology, blood SDF-1 may function as a pro-survival factor. The mechanism(s) responsible for CXCR7 induction and CXCR4 down-regulation are unknown and beyond the scope of this report. However, prior study found that there are NF-κB binding sites in the *CXCR7* gene promoter (23). Thus, it is conceivable that in our system, PMA or IFN-γ plus LPS activated the NF-κB pathway, leading to CXCR7 gene induction.

Debate continues regarding whether CXCR7 acts as a signaling or non-signaling "decoy" receptor (8, 24). In general, two models have been proposed: 1) CXCR7 is a non-signaling receptor and functions as a scavenger to remove extracellular SDF-1, thereby indirectly controlling CXCR4 signaling(25–28); 2) CXCR7 acts as typical signaling receptor either as an independent entity or via hetero-dimerization with CXCR4 (29–35). Of note, even for dimerization, both positive and negative impacts of CXCR7 on CXCR4 signaling have been reported (29, 30, 34). Currently, there is no clear explanation for these contradictions; however, cell type or cell context difference may be a contributing factor. In the current study, we found that the up-regulated CXCR7 receptor is a functional signaling receptor at least during monocyte-to-macrophage differentiation. Several lines of evidence support this notion: 1) SDF-1 activated p38 and JNK pathways in differentiating macrophages bearing both CXCR4 and CXCR7 receptors; 2) In monocytes expressing only CXCR4, SDF-1 was unable to activate p38 and JNK; 3) The effect of SDF-1 on p38/JNK in macrophages was fully mimicked by the CXCR7-selective agonist TC14012; and 4) siRNA silencing of *CXCR7*, but not *CXCR4*, abolished SDF-1-induced p38 and JNK activation. Thus, we provide strong evidence indicating that CXCR7 is required for SDF-1 signaling to p38 and

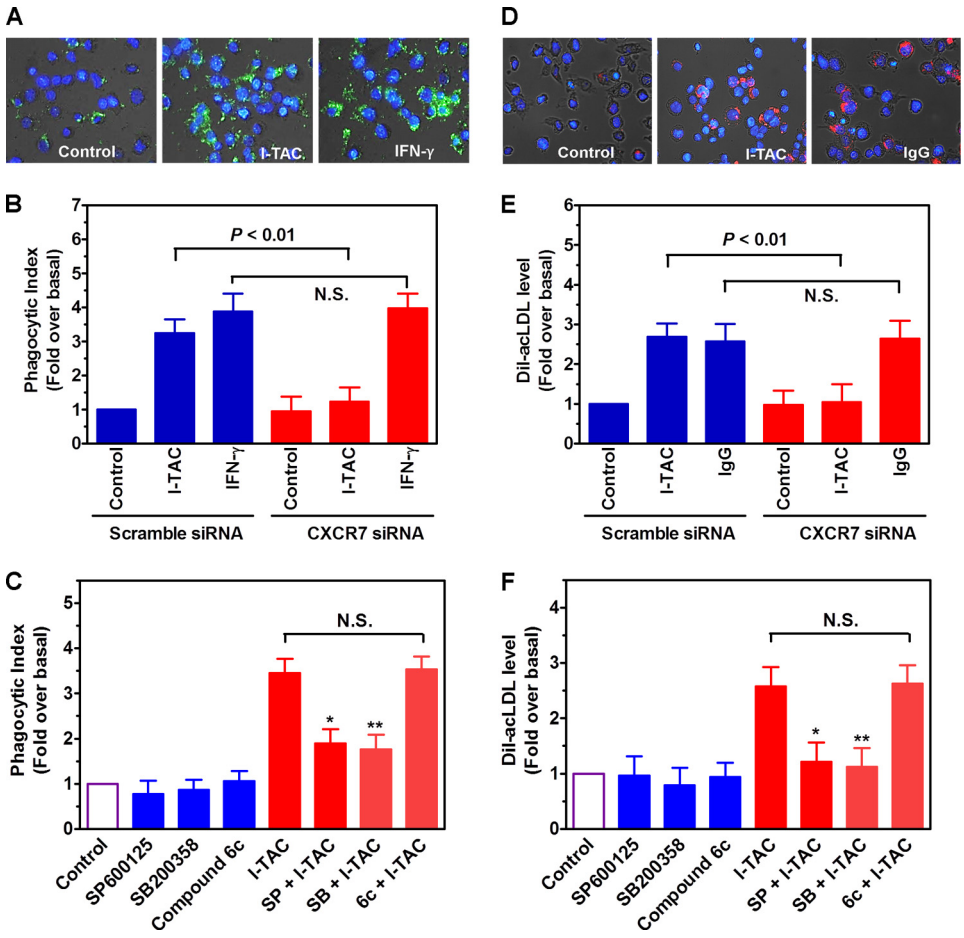

FIGURE 9. **Role of CXCR7 in I-TAC-induced macrophage phagocytosis.** *A*, THP-1 macrophages were starved and activated by vehicle (control), I-TAC (100 ng/ml), or IFN-γ (100 ng/ml) for 2 h, after which FITC-labeled *E. coli* were added and further incubated for 2 h. Then phagocytic index was determined by measuring green fluorescence intensity emitted by the uptaken particles. Shown are merged images of macrophages (phase contrast) with internalized FITC-*E. coli* particles (*green*) and DAPI-positive nuclei (*blue*). Image magnification: ×20. *B*, effect of CXCR7 knockdown by siRNA on I-TAC- or IFN-γ-induced phagocytic activities in THP-1 macrophages. *N.S.* stands for statistic non-significance. $n = 5$. *C*, after pretreating the cells with or without SP600125 (30 μM), SB200358 (10 μM), or compound 6c (10 μM) for 40 min, cells were stimulated by I-TAC (100 ng/ml) for 2 h. Then phagocytosis assay was performed as described above. *, $p < 0.05$; **, $p < 0.01$ compared with the corresponding controls, $n = 5$. *D*, effect of I-TAC and IgG (FcγR agonist) on the uptake of Dil-acLDL in THP-1 macrophages. Image magnification: ×20. *E*, effect of CXCR7 knockdown by siRNA on I-TAC (100 ng/ml)- or IgG (50 μg/ml)-induced uptake of Dil-acLDL in THP-1 macrophages. *N.S.* stands for statistic non-significance, $n = 5$. *F*, after pretreating the cells with or without SP600125 (30 μM), SB200358 (10 μM) or compound 6c (10 μM) for 40 min, cells were stimulated by I-TAC (100 ng/ml) for 2 h. Then Dil-acLDL uptake was measured as described in "Experimental Procedures." *, $p < 0.05$; **, $p < 0.01$ compared with the controls, $n = 5$.

JNK pathways and CXCR4 is dispensable in this process in macrophages. This interpretation is further supported by our finding that I-TAC, which does not bind to CXCR4, can activate p38 and JNK pathways as well in a CXCR7-dependent, but CXCR3-independent manner in macrophages.

The *in vivo* relevance of our findings to the pathogenesis of atherosclerosis can be envisioned in several aspects: 1) We found that SDF-1 activates the pro-survival ERK and AKT pathways, but not the pro-inflammatory p38 and JNK pathways in primary blood monocytes. This result implies that normal blood level of SDF-1 may be beneficial for vascular homeostasis through nurturing blood monocytes and keeping them inside bloodstream via CXCR4 signaling; 2) once blood SDF-1 moves down to the threshold level, blood monocytes may be more prone to emigrate into sub-endothelial space and differentiate into macrophages. During this process, CXCR4 is down-regulated and CXCR7 is up-regulated, the latter of which may promote vascular inflammation by activation of the pro-inflammatory p38 and JNK pathways; 3) our data clearly show that CXCR7 is detectable in aortic atheroma of *ApoE*-null, but not normal, mice, with a restricted expression in macrophage-positive area, suggesting a potential involvement of macrophage CXCR7 in atherogenesis; and 4) we found that activation of CXCR7 increased phagocytosis (uptake of bacterial and modified LDL), evidently mediated by the p38 and JNK pathways, since blocking either of these two pathways has a negative impact on cellular phagocytosis. However, macrophage phagocytosis is a complicated process that involves a variety of receptors, signaling pathways and cytoskeleton proteins (2). The mechanisms of uptake *E. coli* and modified-LDL are not exactly the same, but it is generally believed that the scavenger receptor SR-A participates in both types of phagocytosis. SR-A also mediates macrophage efferocytosis, but others like SR-B, LOX-1, CD68, and CD14 play a role as well (2). It will be of interest to determine whether CXCR7 employs the same or different mechanism(s) to promote uptake of bacterial *versus* modified-LDL. Nonetheless, given the fact that both SDF-1 and I-TAC promote macrophage phagocytosis in a CXCR7-depen-

dent manner, it is imperative to further study the role of CXCR7 in macrophage biology.

In summary, we report the first evidence that during monocyte-to-macrophage differentiation, CXCR7 is induced while CXCR4 is down-regulated. Also, CXCR7 is primarily responsible for SDF-1 and I-TAC stimulation of pro-inflammatory signaling pathways such as JNK and p38, leading to enhanced capability of macrophage phagocytosis. These findings suggest that SDF-1 may play dual roles in atherosclerosis via its two receptors. This concept is supported by a recent study showing that *in vivo* delivery of CXCR4 antagonist exaggerates atherosclerosis (7). In addition, identification of CXCR7 activation of JNK and p38 pathways may also have significant implications for better understanding of the role of CXCR7 in other cells expressing this receptor. Furthermore, future studies using conditional *CXCR7*-null mice may provide a better understanding of *in vivo* roles of this receptor in vascular and leukocyte biology.

REFERENCES

1. Wenner Moyer, M. (2010) The search beyond statins. *Nat. Med.* **16,** 150–153
2. Ley, K., Miller, Y. I., and Hedrick, C. C. (2011) Monocyte and macrophage dynamics during atherogenesis. *Arterioscler. Thromb. Vasc. Biol.* **31,** 1506–1516
3. Gautier, E. L., Jakubzick, C., and Randolph, G. J. (2009) Regulation of the migration and survival of monocyte subsets by chemokine receptors and its relevance to atherosclerosis. *Arterioscler. Thromb. Vasc. Biol.* **29,** 1412–1418
4. Abi-Younes, S., Sauty, A., Mach, F., Sukhova, G. K., Libby, P., and Luster, A. D. (2000) The stromal cell-derived factor-1 chemokine is a potent platelet agonist highly expressed in atherosclerotic plaques. *Circ. Res.* **86,** 131–138
5. Wei, D., Wang, G., Tang, C., Qiu, J., Zhao, J., Gregersen, H., and Deng, L. (2012) Upregulation of SDF-1 is associated with atherosclerosis lesions induced by LDL concentration polarization. *Ann. Biomed. Eng.* **40,** 1018–1027
6. Damås, J. K., Waehre, T., Yndestad, A., Ueland, T., Müller, F., Eiken, H. G., Holm, A. M., Halvorsen, B., Frøland, S. S., Gullestad, L., and Aukrust, P. (2002) Stromal cell-derived factor-1alpha in unstable angina: potential antiinflammatory and matrix-stabilizing effects. *Circulation* **106,** 36–42
7. Zernecke, A., Bot, I., Djalali-Talab, Y., Shagdarsuren, E., Bidzhekov, K., Meiler, S., Krohn, R., Schober, A., Sperandio, M., Soehnlein, O., Bornemann, J., Tacke, F., Biessen, E. A., and Weber, C. (2008) Protective role of CXC receptor 4/CXC ligand 12 unveils the importance of neutrophils in atherosclerosis. *Circ. Res.* **102,** 209–217
8. Sun, X., Cheng, G., Hao, M., Zheng, J., Zhou, X., Zhang, J., Taichman, R. S., Pienta, K. J., and Wang, J. (2010) CXCL12 / CXCR4 / CXCR7 chemokine axis and cancer progression. *Cancer Metastasis. Rev.* **29,** 709–722
9. Burns, J. M., Summers, B. C., Wang, Y., Melikian, A., Berahovich, R., Miao, Z., Penfold, M. E., Sunshine, M. J., Littman, D. R., Kuo, C. J., Wei, K., McMaster, B. E., Wright, K., Howard, M. C., and Schall, T. J. (2006) A novel chemokine receptor for SDF-1 and I-TAC involved in cell survival, cell adhesion, and tumor development. *J. Exp. Med.* **203,** 2201–2213
10. Sierro, F., Biben, C., Martínez-Muñoz, L., Mellado, M., Ransohoff, R. M., Li, M., Woehl, B., Leung, H., Groom, J., Batten, M., Harvey, R. P., Martínez, A. C., Mackay, C. R., and Mackay, F. (2007) Disrupted cardiac development but normal hematopoiesis in mice deficient in the second CXCL12/SDF-1 receptor, CXCR7. *Proc. Natl. Acad. Sci. U.S.A.* **104,** 14759–14764
11. Ma, Q., Jones, D., Borghesani, P. R., Segal, R. A., Nagasawa, T., Kishimoto, T., Bronson, R. T., and Springer, T. A. (1998) Impaired B-lymphopoiesis, myelopoiesis, and derailed cerebellar neuron migration in CXCR4- and SDF-1-deficient mice. *Proc. Natl. Acad. Sci. U.S.A.* **95,** 9448–9453
12. Berahovich, R. D., Zabel, B. A., Penfold, M. E., Lewén, S., Wang, Y., Miao, Z., Gan, L., Pereda, J., Dias, J., Slukvin, II, McGrath, K. E., Jaen, J. C., and Schall, T. J. (2010) CXCR7 protein is not expressed on human or mouse leukocytes. *J. Immunol.* **185,** 5130–5139
13. Shen, J., Chandrasekharan, U. M., Ashraf, M. Z., Long, E., Morton, R. E., Liu, Y., Smith, J. D., and DiCorleto, P. E. (2010) Lack of mitogen-activated protein kinase phosphatase-1 protects ApoE-null mice against atherosclerosis. *Circ. Res.* **106,** 902–910
14. Xu, Q., Wang, J., He, J., Zhou, M., Adi, J., Webster, K. A., and Yu, H. (2011) Impaired CXCR4 expression and cell engraftment of bone marrow-derived cells from aged atherogenic mice. *Atherosclerosis* **219,** 92–99
15. Berahovich, R. D., Penfold, M. E., and Schall, T. J. (2010) Nonspecific CXCR7 antibodies. *Immunol. Lett.* **133,** 112–114
16. Gravel, S., Malouf, C., Boulais, P. E., Berchiche, Y. A., Oishi, S., Fujii, N., Leduc, R., Sinnett, D., and Heveker, N. (2010) The peptidomimetic CXCR4 antagonist TC14012 recruits beta-arrestin to CXCR7: roles of receptor domains. *J. Biol. Chem.* **285,** 37939–37943
17. DiPersio, J. F., Micallef, I. N., Stiff, P. J., Bolwell, B. J., Maziarz, R. T., Jacobsen, E., Nademanee, A., McCarty, J., Bridger, G., and Calandra, G. (2009) Phase III prospective randomized double-blind placebo-controlled trial of plerixafor plus granulocyte colony-stimulating factor compared with placebo plus granulocyte colony-stimulating factor for autologous stem-cell mobilization and transplantation for patients with non-Hodgkin's lymphoma. *J. Clin. Oncol.* **27,** 4767–4773
18. Fricker, S. P. (2008) A novel CXCR4 antagonist for hematopoietic stem cell mobilization. *Expert. Opin. Investig. Drugs* **17,** 1749–1760
19. Balabanian, K., Lagane, B., Infantino, S., Chow, K. Y., Harriague, J., Moepps, B., Arenzana-Seisdedos, F., Thelen, M., and Bachelerie, F. (2005) The chemokine SDF-1/CXCL12 binds to and signals through the orphan receptor RDC1 in T lymphocytes. *J. Biol. Chem.* **280,** 35760–35766
20. Tarnowski, M., Liu, R., Wysoczynski, M., Ratajczak, J., Kucia, M., and Ratajczak, M. Z. (2010) CXCR7: a new SDF-1-binding receptor in contrast to normal CD34(+) progenitors is functional and is expressed at higher level in human malignant hematopoietic cells. *Eur. J. Haematol.* **85,** 472–483
21. Infantino, S., Moepps, B., and Thelen, M. (2006) Expression and regulation of the orphan receptor RDC1 and its putative ligand in human dendritic and B cells. *J. Immunol.* **176,** 2197–2207
22. Seeger, F. H., Tonn, T., Krzossok, N., Zeiher, A. M., and Dimmeler, S. (2007) Cell isolation procedures matter: a comparison of different isolation protocols of bone marrow mononuclear cells used for cell therapy in patients with acute myocardial infarction. *Eur. Heart J.* **28,** 766–772
23. Tarnowski, M., Grymula, K., Reca, R., Jankowski, K., Maksym, R., Tarnowska, J., Przybylski, G., Barr, F. G., Kucia, M., and Ratajczak, M. Z. (2010) Regulation of expression of stromal-derived factor-1 receptors: CXCR4 and CXCR7 in human rhabdomyosarcomas. *Mol. Cancer Res.* **8,** 1–14
24. Thelen, M., and Thelen, S. (2008) CXCR7, CXCR4 and CXCL12: an eccentric trio? *J Neuroimmunol.* **198,** 9–13
25. Naumann, U., Cameroni, E., Pruenster, M., Mahabaleshwar, H., Raz, E., Zerwes, H. G., Rot, A., and Thelen, M. (2010) CXCR7 functions as a scavenger for CXCL12 and CXCL11. *PLoS One* **5,** e9175
26. Luker, K. E., Steele, J. M., Mihalko, L. A., Ray, P., and Luker, G. D. (2010) Constitutive and chemokine-dependent internalization and recycling of CXCR7 in breast cancer cells to degrade chemokine ligands. *Oncogene* **29,** 4599–4610
27. Boldajipour, B., Mahabaleshwar, H., Kardash, E., Reichman-Fried, M., Blaser, H., Minina, S., Wilson, D., Xu, Q., and Raz, E. (2008) Control of chemokine-guided cell migration by ligand sequestration. *Cell* **132,** 463–473
28. Wang, H., Beaty, N., Chen, S., Qi, C. F., Masiuk, M., Shin, D. M., and Morse, H. C., 3rd (2012) The CXCR7 chemokine receptor promotes B-cell retention in the splenic marginal zone and serves as a sink for CXCL12. *Blood* **119,** 465–468
29. Décaillot, F. M., Kazmi, M. A., Lin, Y., Ray-Saha, S., Sakmar, T. P., and Sachdev, P. (2011) CXCR7/CXCR4 heterodimer constitutively recruits beta-arrestin to enhance cell migration. *J. Biol. Chem.* **286,** 32188–32197
30. Levoye, A., Balabanian, K., Baleux, F., Bachelerie, F., and Lagane, B. (2009) CXCR7 heterodimerizes with CXCR4 and regulates CXCL12-mediated G protein signaling. *Blood* **113,** 6085–6093

31. Odemis, V., Lipfert, J., Kraft, R., Hajek, P., Abraham, G., Hattermann, K., Mentlein, R., and Engele, J. (2012) The presumed atypical chemokine receptor CXCR7 signals through G(i/o) proteins in primary rodent astrocytes and human glioma cells. *Glia* **60,** 372–381
32. Hartmann, T. N., Grabovsky, V., Pasvolsky, R., Shulman, Z., Buss, E. C., Spiegel, A., Nagler, A., Lapidot, T., Thelen, M., and Alon, R. (2008) A crosstalk between intracellular CXCR7 and CXCR4 involved in rapid CXCL12-triggered integrin activation but not in chemokine-triggered motility of human T lymphocytes and CD34+ cells. *J. Leukoc. Biol.* **84,** 1130–1140
33. Odemis, V., Boosmann, K., Heinen, A., Küry, P., and Engele, J. (2010) CXCR7 is an active component of SDF-1 signalling in astrocytes and Schwann cells. *J. Cell Sci.* **123,** 1081–1088
34. Zabel, B. A., Wang, Y., Lewén, S., Berahovich, R. D., Penfold, M. E., Zhang, P., Powers, J., Summers, B. C., Miao, Z., Zhao, B., Jalili, A., Janowska-Wieczorek, A., Jaen, J. C., and Schall, T. J. (2009) Elucidation of CXCR7-mediated signaling events and inhibition of CXCR4-mediated tumor cell transendothelial migration by CXCR7 ligands. *J. Immunol.* **183,** 3204–3211
35. Rajagopal, S., Kim, J., Ahn, S., Craig, S., Lam, C. M., Gerard, N. P., Gerard, C., and Lefkowitz, R. J. (2010) Beta-arrestin- but not G protein-mediated signaling by the "decoy" receptor CXCR7. *Proc. Natl. Acad. Sci. U.S.A.* **107,** 628–632
36. Schnoor, M., Buers, I., Sietmann, A., Brodde, M. F., Hofnagel, O., Robenek, H., and Lorkowski, S. (2009) Efficient non-viral transfection of THP-1 cells. *J. Immunol. Methods* **344,** 109–115